Cold Crucible Vitrification and Characterization of Vitrified Savannah River Sludge Batch 4 Waste Surrogate - 10139

S.V. Stefanovsky*, V.V. Lebedev*, M.A. Polkanov*, D.Y. Suntsov*, J.C. Marra**
* SIA Radon, 7th Rostovskii lane 2/14, Moscow 119121 RUSSIA, profstef@mtu-net.ru
** Savannah River National Laboratory, Building 773-A, Aiken, SC 29808 USA

ABSTRACT

In the frame of collaborative work between SRNL and Daymos/SIA Radon crystal settling/formation in borosilicate melts with high iron and aluminum contents produced from Sludge Batch 4 (SB4) high level waste (HLW) surrogate and commercially available Frit 503-R4 by cold crucible inductive melting (CCIM) was studied. The melts at 55 wt.% waste loading were produced in 236 mm inner diameter cold crucible and kept at a temperature of ~1300 °C for ~30, ~40, ~60 and ~90 min to evaluate the effect of melt keeping on homogeneity and crystal settling/formation in the as-poured and solidified melts. After keeping for certain time melt was poured into 10 L heat-insulated canisters where glassy materials were slowly cooled / annealed. Average slurry feed and glass production rates are influenced by melt viscosity, including viscosity vs temperature dependence, and electric resistivity. At >50 wt.% waste loading in glass the melts become non-Newton liquids and deviation from the Frenkel-Andrade's law increases with the increase of waste loading. This means the glass becomes structured and structuring effects on process variables. Exhausts of aerosols and gas constituents normally occur during slurry feeding while the lowest values are typical during melt keeping and pouring. Among off-gas constituents the highest concentrations were found for nitrogen oxides – NO and NO_2 which are released at decomposition of sodium nitrite and nitrate. Concentrations and release rates of CO, HCl and F are much lower. Low concentrations and release rates of SO_2 are due to its volatilization mainly in an aerosol form. X-ray diffraction, optical microscopy, electron microscopy, and infra-red spectroscopic studies did not reveal appreciable difference in the texture of the materials obtained from the melts kept in the cold crucible for various times. Glass blocks are composed of vitreous and spinel structure phases. Spinel is present as both skeleton-type aggregates of fine (micron- or submicron-sized) crystals segregated at early stages of melt solidification and larger (up to tens of microns) individual more regular crystals formed during slow melt cooling. There is a some tendency to elemental separation in the glass blocks with enrichment of the deeper zones with heavier transition metal ions and their depletion with Na, Cs, Ca, Al, Si.

INTRODUCTION

SIA Radon performed testing that has demonstrated the feasibility of the Cold Crucible Induction Melter (CCIM) to achieve high waste loadings and maintain high throughput for Savannah River Site high-level waste (HLW) feeds. A full-scale demonstration using 418 mm inner diameter cold crucible with the high alumina content SB4 feed was completed with a waste loading of 50 wt % [1]. In the bench-scale test a practical limit for waste loading with the SB4 composition has been determined to be ~55 wt.% [2]. Additionally, prior to implementation of a CCIM in a production process it is necessary to better understand processing constraints with the CCIM. The glass liquidus temperature requirement for processing in the CCIM is an open issue. The current specification for waste glass processing in the Defense Waste Processing Facility (DWPF) Joule Heated Melter (JHM) is the $T_{melt\ temp.} - T_{liquidus} \geq 100°$ C. There appears to be no specific liquidus temperature criterion for CCIM processing. In long-term operation, the potential for crystal settling and/or build-up in the CCIM must be considered as well as the potential for adverse effects on melter processing or operations (e.g. pouring). Therefore, a specific criterion for liquidus temperature needs to be established. Finally, an evaluation of melt homogeneity as a function of residence time in the cold crucible and glassy product homogeneity are needed to assess product consistency considerations and to evaluate product quality during upset conditions.

EXPERIMENTAL

The test was performed at the Radon bench-scale facility equipped with a 236 mm inner diameter stainless steel cold crucible described elsewhere [2].
The SB4 sludge surrogate (Table 1) was prepared by a SRT-MST-2007-00070 procedure [3]. It was intermixed with a Frit 503-R4 (wt.%: 8 Li_2O, 16 B_2O_3, 76 SiO_2) to obtain a slurry with a water content of ~50 wt.%. The slurry calculated to obtain a glass at 55 wt.% waste loading was prepared in amount of ~281 kg in 12 containers. Calculated chemical composition of the glass was as follows, wt.%: Al_2O_3 – 14.66, BaO – 0.04, CaO – 1.62, Cr_2O_3 – 0.12, CuO – 0.03, Fe_2O_3 – 16.65, K_2O – 0.04, MgO – 1.63; MnO – 3.31, Na_2O – 11.59, NiO – 0.95, PbO – 0.21, SiO_2 – 35.77, ZnO – 0.03, ZrO_2 – 0.05, Cs_2O – 0.55, F – 0.02, Cl – 1.33, I – 0.03, P_2O_5 – 0.18, SO_3 – 0.39, B_2O_3 – 7.20, Li_2O – 3.60. Cesium was introduced as a $CsNO_3$ in amount of 0.55 wt.% Cs_2O.

Table I. Expected Concentration of Anion/Cation Content of SB4 Feed Simulant (Final Product).

Cation	wt% total solids	wt % calcined solids	Cation	wt% total solids	wt % calcined solids	Anion	Concentra-tion, g/L
Al^{3+}	10.381	14.830	Mg^{2+}	1.287	1.839	SO_4^{2-}	1.386
Ba^{2+}	0.048	0.069	Mn^{2+}	3.447	4.924	PO_4^{3-}	0.284
Ca^{2+}	1.521	2.172	Na^{+}	10.679	15.256	CO_3^{2-}	7.449
Ce^{3+}	0.141	0.201	Ni^{2+}	1.004	1.434	SO_4^{2-}	1.319
Cr^{3+}	0.104	0.149	Pb^{2+}	0.273	0.390	NO_3^{-}	5.595
Cu^{2+}	0.031	0.045	Si	0.975	1.393	Cl^{-}	3.550
Fe^{3+}	15.602	22.289	Zn^{2+}	0.031	0.044	F^{-}	0.045
K^{+}	0.043	0.062	Zr^{4+}	0.052	0.074	I^{-}	0.085
						NO_2^{-}	13.762
						OH^{-}	5.158
Specific Gravity, g/mL			1.14	Total Organic Carbon (TOC)			<0.05
Total Solids, wt. %			20	Total Solids, g			276.0
Soluble Solids, wt. %			4.72%	Estimated Calcine Factor			0.7

The CCIM test was performed in 4 steps for totally 51 hrs. 15 min.:

1) Process start-up and operation melt volume production;
2) Achieving of target glass composition in the cold crucible;
3) SB4 waste surrogate vitrification;
4) Process stopping and melter cooling.

During Step 1 the glass breakage with approximate 60 wt.% waste loading from the previous test in amount of 10.8 kg and 1.8 kg of batch normally applied at SIA Radon to CCIM process start-up were fed into the cold crucible. After completion of starting melt formation the SB4 waste slurry in amount of 18.9 kg was fed for 3 hrs. 32 min. The glass produced was poured in amount of 10.6 kg into canister #0 and a portion of the glassmelt was sampled into a mold #0.

During the step 2 starting melt with ~60 wt.% SB4 waste loading was completely substituted by the glass with target composition at 55 wt.% SB4 waste loading for 29 hrs. 41 min at average input power at slurry feeding and melt homogenization of 29.6 kW and 44.6 kW, respectively. Variation in input power during the step 2 is shown on Fig. 1(upper). Glassmelt was poured into 10 L canisters ## 1 to 3. A portion of glassmelt was sampled into a mold #0.

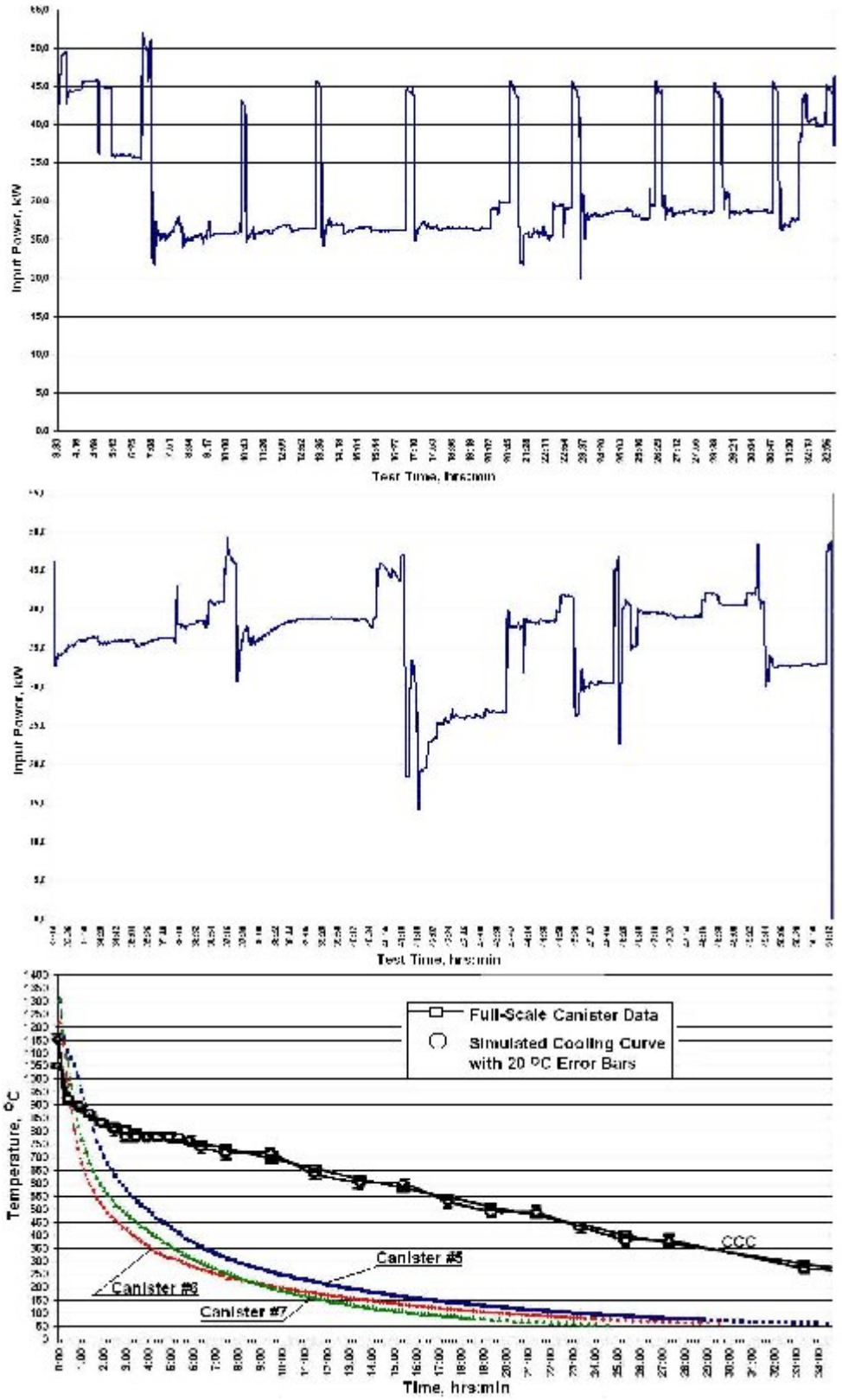

Figure 1. Variations in Input Power during the Steps 2 (upper) and 3 (middle) and Cooling Curves for the Glasses in Canisters ## 5-7 and Actual and Simulated Canister Centerline Cooling (CCC) Curves [4] (lower).

During the step 3 (duration 18 hrs. 2 min) average input power at slurry feeding and melt homogenization were 36.1 kW and 39.2 kW, respectively. Variation in input power during the step 3 is shown on Fig. 1 (middle). Glassmelt was poured into 10 L canisters ## 4 to 7. At that, portions of glassment were sampled into molds ##1 to 4 (Fig. 2, upper left).

Before pouring from the cold crucible melt was kept for ~15, ~30, ~60 and ~90 min to evaluate the effect of melt holding on its homogeneity and crystal settling/formation in the as-poured and solidified melts. After keeping for certain time melt was poured into heat-insulated canisters (Fig. 2, upper right) where glassy materials were cooled by regimes shown on Fig. 1 (lower).

In the whole, during the steps 2 and 3 the slurry in amount of 246.8 kg was processed and glassy material in amount of 102.9 kg was produced for 47 hrs 45 min. The diagram demonstrating the dynamics of slurry processing and glass production is shown on Fig. 2 (lower). Major process variables are given in Table II.

Table II. Major CCIM Process Variables.

Major Process Variables	Canister #			
	4	5	6	7
Average vibration power, kW	46.5			
Mass of the glass produced, kg	35.2			
Slurry feed rate (excluding time spent for melt homogenization and pour), kg/hr	6.6			
Glass production rate (excluding time spent for melt holding and pour), kg/hr	2.5			
Time spent for melt holding and pour, min	30	40	64	92
Glass production rate (including time spent for melt holding and pour), kg/hr	1.7	1.5	1.2	1.0
Melting ratio, kW×hr/kg	27.4	31.0	38.8	46.5
Specific glass production rate, kg/(m^2×d)	932.7	823.0	658.4	548.7

Variations in input power during the SB4 waste surrogate vitrification process are typical of the CCIM and reflect cyclic character of the process consisting of slurry feeding, melt homogenization and pouring [1,2]. Values of average slurry feed (6.6 kg/hr) and glass production rates (2.5 kg/hr) are some lower than those obtained in the previous test (~8.2 kg/hr and ~3.6 kg/hr) at 60 wt.% SB4 waste loading in glass [2]. The reasons may be in some properties of glassmelts such as electric resistivity and viscosity including temperature dependence of viscosity (Table III).

Visualization of the effect of temperature on viscosity of molten glass in the co-ordinates $\log_{10}\eta$ — 1/T (Fig. 3) shows that the only glass at 50 wt.% SB4 waste loading on its viscous properties is close to the Newton type liquid and its $\log_{10}\eta$ — 1/T dependence obeys Frenkel-Andrade's law. At higher waste loadings in glass their melts become non-Newton liquids and deviation from the Frenkel-Andrade's law increases with the increase of waste loading (Fig. 3).

Such behavior of molten glasses at high waste loadings is typical of structured liquids and takes place due to elevated content of crystalline phase which is mainly spinel but nepheline may be also present. In our previous works (see [1,2]) we esimated the degree of crystallinity in the glassy material ~6.5 vol.% at ~55 wt.% and ~12.0 vol.% at ~60 wt.% SB4 waste loadings. As follows from reference data [5] appreciable structurization occurs at solid phase content ≥30 vol.% if particles are spherical and ~20 vol.% if particles have irregular form (non-spherical). As seen from Fig. 3, significant deviaion from the linear dependence $\log_{10}\eta$ — 1/T occurs already at ~55 wt.% waste loading and ~6.5 vol.% crystalline phase in glass. One of the possible explanations is that method of determination of the degree of crystallinity using Corel Photo-

Paint software is in error on the low side. Another reason is occurrence of microcrystalline nepheline having color similar to glass and undistinguishable on its background.

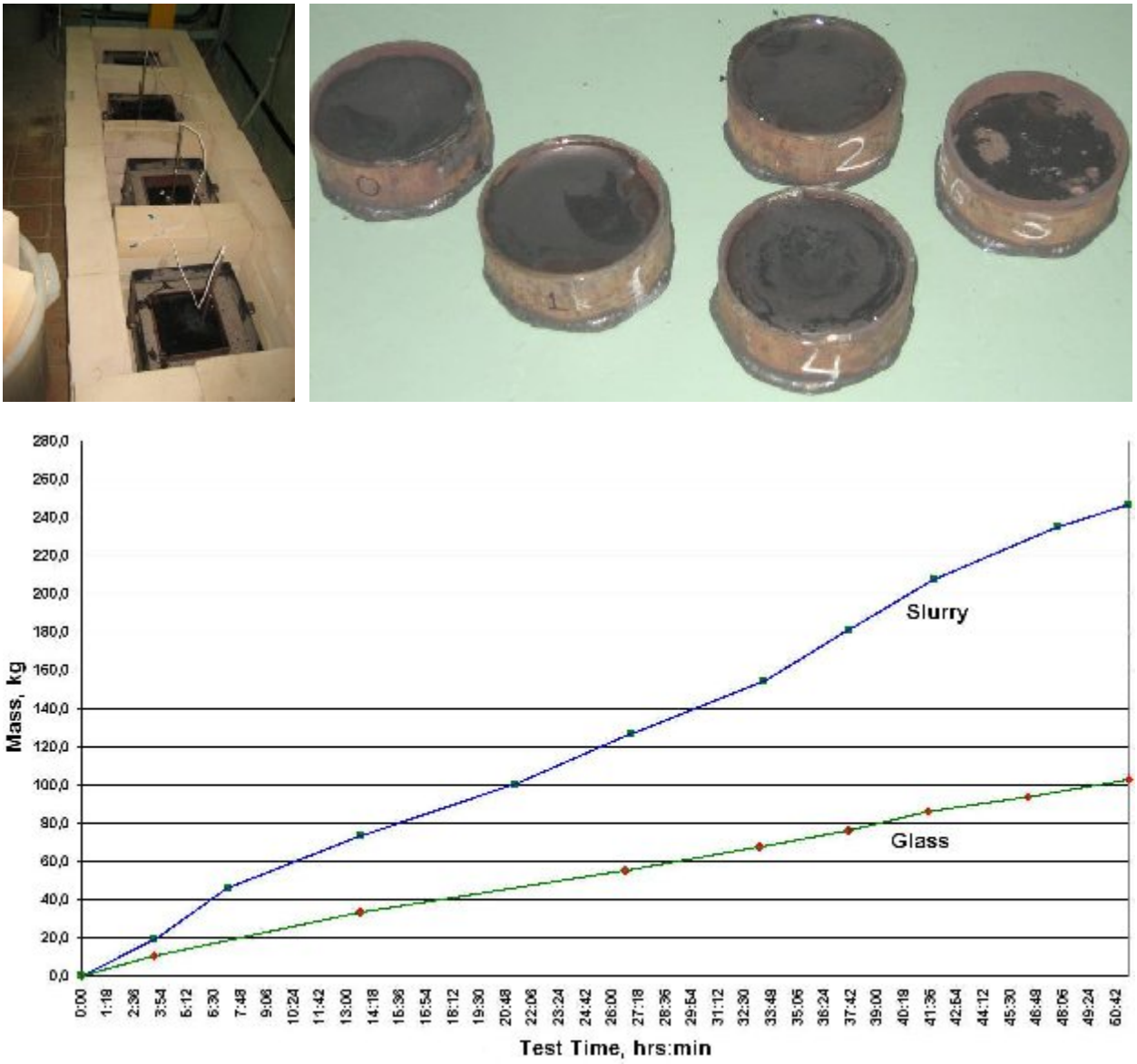

Figure 2. View of Heat-Insulated (Asbestos Cover is Removed) Canisters ## 4-7 with Solidified Glass Produced during Step 3 (upper left) and Molds with Glass Sampled during Pouring into Canisters (upper right) and the Dynamics of Slurry Processing and Glass Production during the Test.

The test was stopped after complete pouring of the last portion of molten glass to pouring level at 52th hour of operation. Further cooling of the melter (Step 4) took ~2 hrs followed by complete de-energization of all the equipment.

The cold crucible operated for ~52 hrs and ~103 kg of molten glass was poured through the pouring unit. No appreciable traces of corrosion of crucible and pouring unit construvtion material were found. Both the melter and pouring unit are suitable for further operation.

Table III. Effect of Temperature on Viscosity of Glassmelts (Poise) at Various Waste Loadings.

Temperature, °C	Waste loading, wt.%		
	50	55	60
1200	88.2	-	-
1250	63.7	5520	-
1300	49.5	830	$179 \cdot 10^4$
1350	32.5	21.5	173.5
1400	22.5	18.4	16.5
1450	17.5	13.8	7.5

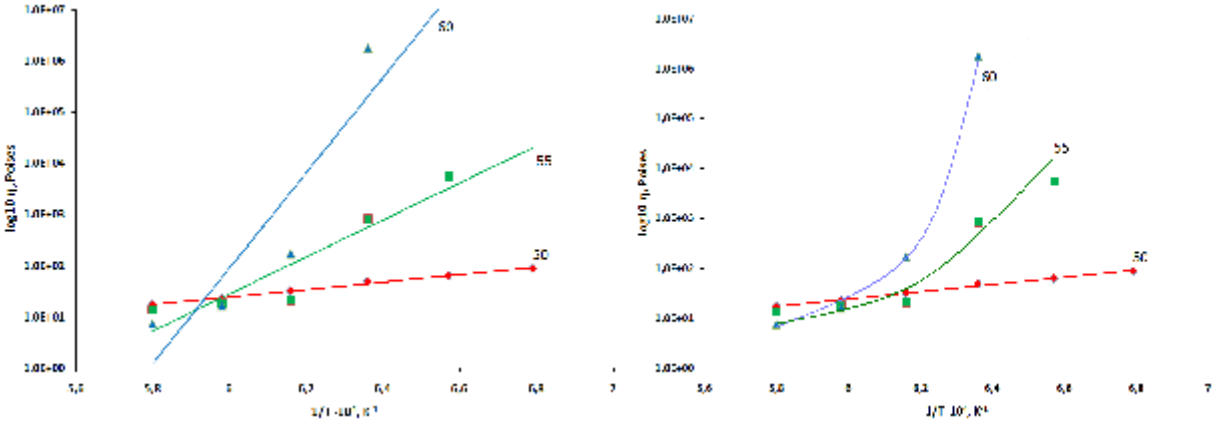

Figure 3. The Dependences of Viscosity from Temperature for the Glasses at Various Waste Loadings with Trends Obeying to the Frenkel-Andrade's Law and the Actual Dependences of Viscosity from Temperature for the Glasses at Various Waste Loadings.

OFF-GAS ANALYSES

During the bench-scale CCIM test flow rates of off-gas and air dispensed through heater to dilute off-gas from the melter were measured. Off-gas was analyzed to determine CO, NO_2, NO, SO_2, HCl, F^-, and aerosols. Off-gas and compressed air flow rates were measured using a DMC-01M differential manometer and a RAMC rotameter, respectively. CO, NO, NO_2, and SO_2 concentrations were determined using a "Kaskad-512" gas analyzer. HCl concentration was measured by a standard technique with $AgNO_3$. Concentration of fluoride ions was measured by a photocolorimetric method with lanthanum alizarin complexing agent. SO_2 concentration was also measured using a technique with $Pb(NO_3)_2$. Aerosols were determined by a weighing procedure. Average off-gas parameters are listed in Table IV.

Exhausts of aerosols and gas constituents normally occur during slurry feeding while the lowest values are typical during melt keeping and pouring. Among off-gas constituents the highest concentrations were found for nitrogen oxides – NO and NO_2 which are released at decomposition of sodium nitrite ($NaNO_2$) and nitrate ($NaNO_3$). Concentrations and release rates of CO and HCl are much lower. Fluor is present in the waste surrogate and feed in low concentration and, as a result, its concentration in off-gas is also low. Low concentrations and release rates of SO_2 are due to its volailization mainly in aerosol form [1,2].

GLASS SAMPLING AND ANALYSES

Portions of molten glasses were poured into stainless steel molds. Five molds with glass samples were cooled in air and solidified glass pieces were analyzed by inductive-coupled plasma - atomic absorption

Table IV. Average Off-Gas Parameters during the Test.

Parameters		Aver.	Step1	Step2		Step 3			
				Start	Finish	4	5	6	7
Compressed air flow rate (25 °C, 1 atm), m^3/h		80	80	80	80	80	80	80	80
Off-gas flow rate (25 °C, 1 atm), m^3/h		140	139	143	136	138	136	134	134
Concentration of components in off-gas	[1] NO, $mg(N)/m^3$	741	596	606	870	482	566	2069	1728
	[1] NO_2, $mg(N)/m^3$	194	139	157	243	181	201	519	433
	[1] CO, $mg(C)/m^3$	29	46	28	27	25	25	25	25
	[1] SO_2, $mg(S)/m^3$	4	1	7	0	0	0	0	0
	[2] HCl, mg/m^3	93	165	74	93	nm	nm	96	103
	[2] F^-, mg/m^3	0.36	1.33	0.29	0.37	nm	nm	0.47	0.33
	[3] Aerosols. mg/m^3	250	250	192	210	305	418	117	365
Release rate, g/hr	NO	102	82.6	85.2	129	66.5	75.0	278	230
	NO_2	26.8	19.3	22.2	35.4	24.9	27.2	69.7	57.9
	CO	4.0	6.3	3.9	3.6	3.5	3.4	3.4	3.3
	SO_2	0.6	0.1	1.1	0.0	0.0	0.0	0.0	0.0
	HCl	13.0	22.6	10.6	12.5	nm	nm	12.8	14.3
	F^-	0.050	0.183	0.042	0.049	nm	nm	0.062	0.046
	Aerosols	34	27	30	41	58	61	16	50

[1] "Kaskad-512" gas analyzer, [2] chemical analyses, [3] weighing procedure.

spectroscopy (ICP-AAS) using a Perkin-Elmer 403 spectrometer (at SRNL), X-ray diffraction (XRD) using a DRON-4 diffractometer (Fe Kα radiation), optical microscopy (OM) using an OLYMPUS BX51 polarizing microscope, and scanning electron microscopy with energy dispersive system (SEM/EDS) using a JSM 5610 LV + JED-2300 analytical unit (voltage is 25 KeV, beam current is 1 nA, probe diameter is 1 to 3 μm, dwell time is 100 s; metals, oxides and fluorides were used as standards). Fraction of crystalline phase in the samples was determined using a Corel Photo-Paint 12 software.
Glass in four heat-insulated canisters was spontaneously cooled by a regime shown on Fig. 1(lower). Although these conditions were some different from the CCC conditions [4], certain conclusions on the effect of cooling rate on the types and amounts of crystallization within the glass samples may be done. After cooling ¼ part of each canister was cut out (Fig. 4*a*) and samples for analyses were taken as it is shown on Fig. 4*b*. Moreover, three specimens from "dead volume" of the cold crucible and one specimen of the "skull" (Fig. 4*c*) were sampled and analyzed using the same techniques.

Glassy Products From Molds Sampled At Molten Glass Pouring

Chemical compositions of the glassy products poured in molds as well as the residue from "dead volume" of the cold crucible are given in Table V. Analytical sums for all the glassy products are close to 100 wt.% taking into account that some elements (F, Cl, I, Cs) were not measured.

As follows from XRD, OM and SEM/EDS studies of the glassy products poured in molds and solidified they are composed of major vitreous and spinel structure phases.

General OM features of the glassy materials are as follows:

- Formation of "web" of microcracks (Fig. 23, *1*) pointing to high level of residual thermal stresses in glass in the absence of annealing;
- Color of the lappings of the glassy material depends strongly on glass to spinel ratio; the areas with high sinel content are nearly black and opaque.

Table V. Chemical Compositions (in wt.%) of Glasses Kept in Cold Crucible for Various Times and Poured into Canisters and from "Dead Volume" of Cold Crucible.

Oxide	Target composition*	Kept in cold crucible for a time, min				"Dead volume" (DV)
		15	30	60	90	
Al_2O_3	14.66	15.3	13.4	15.4	15.3	13.1
B_2O_3	7.20	6.96	7.26	6.88	6.84	5.50
BaO	0.04	0.04	0.04	0.04	0.04	0.03
CaO	1.62	1.77	1.76	1.81	1.88	1.32
CeO_2	-	0.00	0.01	0.00	0.00	0.00
Cr_2O_3	0.12	0.11	0.10	0.09	0.10	0.49
CuO	0.03	0.04	0.06	0.06	0.05	0.04
Fe_2O_3	16.65	16.8	14.7	16.6	16.2	26.3
K_2O	0.04	0.06	0.06	0.07	0.08	0.05
Li_2O	3.60	3.17	3.51	3.12	3.08	2.51
MgO	1.63	1.50	1.32	1.51	1.51	1.61
MnO_2	3.31	4.17	3.55	3.82	3.77	4.87
Na_2O	11.59	10.15	10.07	9.95	9.92	8.25
NiO	0.95	0.74	0.66	0.70	0.71	2.42
PbO	0.21	0.12	0.10	0.10	0.11	0.09
SO_3	0.39	0.07	0.09	0.08	0.09	0.27
SiO_2	35.77	38.4	42.0	37.8	38.4	30.4
TiO_2	-	0.04	0.07	0.04	0.05	0.05
ZnO	0.03	0.02	0.03	0.03	0.02	0.04
ZrO_2	0.05	0.09	0.10	0.09	0.09	0.08
Sum	97.89	99.55	98.89	98.19	98.24	97.42

* also contains 0.02 F, 1.33 Cl, 0.03 I, 0.18 P_2O_5, 0.55 Cs_2O; "-" – component was not introduced.

As follows from SEM examination the materials from the molds ## 0, 1, 2, and 4 have the same phase composition and texture. Dendrite spinel crystals are distributed in the vitreous matrix (Fig. 4*d*). Chemical composition of the vitreous phase (Table VI) in various points demonstrates homogeneity of elemental distribution over the bulk. Due to small size of spinel crystals their chemical composition cannot be determined precisely by EDS and capture of surrounding glass takes place. Some elements (P, F, I, Zr) were not determined.

The material sampled from the mold #3 was found to be some non-uniform (Fig. 4*e,f*). There are areas of individual cubic and star-like and dendrite crystals. The areas of the first type have layered texture formed due to frozen laminated flow. The texture of the other areas is same as that of samples from the molds ##0,1, 2, and 4. Relative large sizes of individual crystals in the layered area provide for rather precize determination of their chemical composition (Table VI). Transition metal and aluminum oxides are major components of the spinel phase wheras he vitreous phase is enriched with oxides of alkali elements, mainly Na, Al, Si, and B and Li, which is not determined by EDS. Some elements having very low content in the material were not determined. Analytical sums for he vitreous phase are about 90 wt.%. Boron and lithium oxides account for ~8-10 wt.% of total.

The degree of crystallinity values estimated from SEM images in the materials sampled from the molds ##0, 1, 2, and 4 are similar (~23±3 vol.%). The materal from the mold #3 consists of two areas with different degree of crystallinity: ~20 vol.% in the area of dendrite crystals, and ~12 vol.% in the area of individual crystals. Approximate average degree of crystallinity may be estimated as 16±2 vol.%.

Table VI. Chemical Composition of the Vitreous Phase and Spinel/Glass Aggregates in the Material Sampled from the Molds by SEM/EDS data.

Oxide	#0			#1			#2		#3			#4		
	Scan	V	S+V	Scan	V	S+V	Scan	S+V	V	S+V	S	Scan	V	S+V
Na_2O	12.04	13.01	13.03	12.75	13.05	13.07	13.81	13.10	13.49	6.54	-	12.94	12.92	7.31
MgO	1.70	1.50	1.90	1.88	1.77	1.75	1.86	1.68	1.41	2.80	2.40	1.62	1.36	2.52
Al_2O_3	15.64	18.16	16.02	17.15	19.25	18.37	18.66	20.46	20.05	10.94	4.65	16.58	17.85	10.35
SiO_2	34.50	38.76	28.50	36.08	38.58	33.77	38.09	43.19	42.63	18.14	-	34.33	38.57	16.76
SO_3	*0.11*	*0.17*	-	*0.16*	*0.20*	-	*0.17*	-	0.61	-	-	0.13	0.16	-
Cl	0.27	0.34	-	0.33	0.35	-	0.46	0.54	-	-	-	0.45	0.48	-
K_2O	*0.04*	*0.15*	-	*0.06*	*0.06*	-	*0.13*	*0.10*	2.18	-	-	*0.13*	*0.10*	-
CaO	1.92	2.24	1.43	1.96	2.49	2.00	2.00	2.73	-	-	-	1.82	2.05	0.91
TiO_2	*0.11*	-	-	*0.04*	-	-	-	-	-	-	-	*0.16*	-	-
Cr_2O_3	*0.15*	-	*0.17*	*0.17*	-	*0.18*	*0.13*	-	-	*0.30*	3.58	-	-	0.35
MnO	3.27	2.75	4.01	3.30	2.70	3.62	3.38	3.13	2.73	5.54	5.44	2.72	2.17	5.44
Fe_2O_3	15.16	5.56	28.96	15.57	6.04	17.93	16.24	7.53	7.31	47.31	67.25	12.99	4.52	46.45
NiO	0.74	-	1.27	0.68	-	1.19	0.63	-	-	2.08	8.53	0.49	-	2.07
CuO	*0.03*	*0.02*	-	*0.03*	-	*0.04*	*0.04*	-	-	-	-	-	*0.14*	-
ZnO	0.13	-	0.21	*0.03*	-	*0.04*	*0.14*	-	-	-	-	*0.17*	-	*0.32*
Cs_2O	0.38	0.29	-	0.35	*0.40*	*0.12*	0.23	*0.11*	0.35	-	-	0.27	*0.2*	-
PbO	*0.22*	*0.29*	-	*0.24*	*0.20*	-	*0.19*	-	-	-	-	*0.25*	*0.16*	-
Total	86.41	82.95	95.50	90.78	85.09	92.08	96.20	92.27	90.76	94.68	91.85	85.05	80.68	92.48

Values <2 Sigma are given in Italics; Scan over area of 100×100μm, V – vitreous phase, S – spinel.

Glassy Products From Canisters

As follows from XRD study all the glassy materials sampled from canisters are composed of vitreous and spinel structure phases. The specimens CU, CM, CB, EU, EM, and EB from canister #4 have a texture similar to that observed in the materials sampled from the molds but different in crystal size (Fig. 4*g*) and some variable in chemical composition of the vitreous phase and spinel. Analytical sums for the vitreous phase are normally close to 90 wt.% of total pointing to quite low losses of boron and lithium oxides which are not determined by EDX spectroscopy. Cross size of dendrite spinel crystals in the samples CU and CM is ≤5 μm, that is comparable with electron probe diameter, and, as a result, analyses include captured glass (Tables VII and VIII). Size of the spinel crystals grow towards bottom part of canister where cross size achieves ~10 μm and chemical composition of the spinel crystals may be determined rather precisely.

Dendrite spinel crystals are produced at earlier study of crystallization and relatively faster cooling rate whereas larger individual crystals are typical of slower cooled zones. In the CM, CB, and EB samples crystal size may achieve 30-35 μm (Fig. 4*i*). In the place of contact between the glassy material and canister fayalite crystals with averaged formula $Fe_{1.21}Mn_{0.33}Ni_{0.04}Mg_{0.45}Ca_{0.02}Si_{0.96}Al_{0.03}O_4$ occurred (Table IX). The specimens sampled from the near-bottom area (EB) have, as a rule, a complex texture including areas of chaotically alligned skeleton-type aggregates of fine spinel crystals with rare inclusions of larger-sized individual star-like and cubic crystals and layers of glass containing individual cubic spinel crystals. Although no specific dependence of waste oxides contents from sampling point (Tables IX and X) but there is a tendency to depletion of deeper zones with light elements (Na, Al, Si, Ca) and enrichment with heavier transition metals.

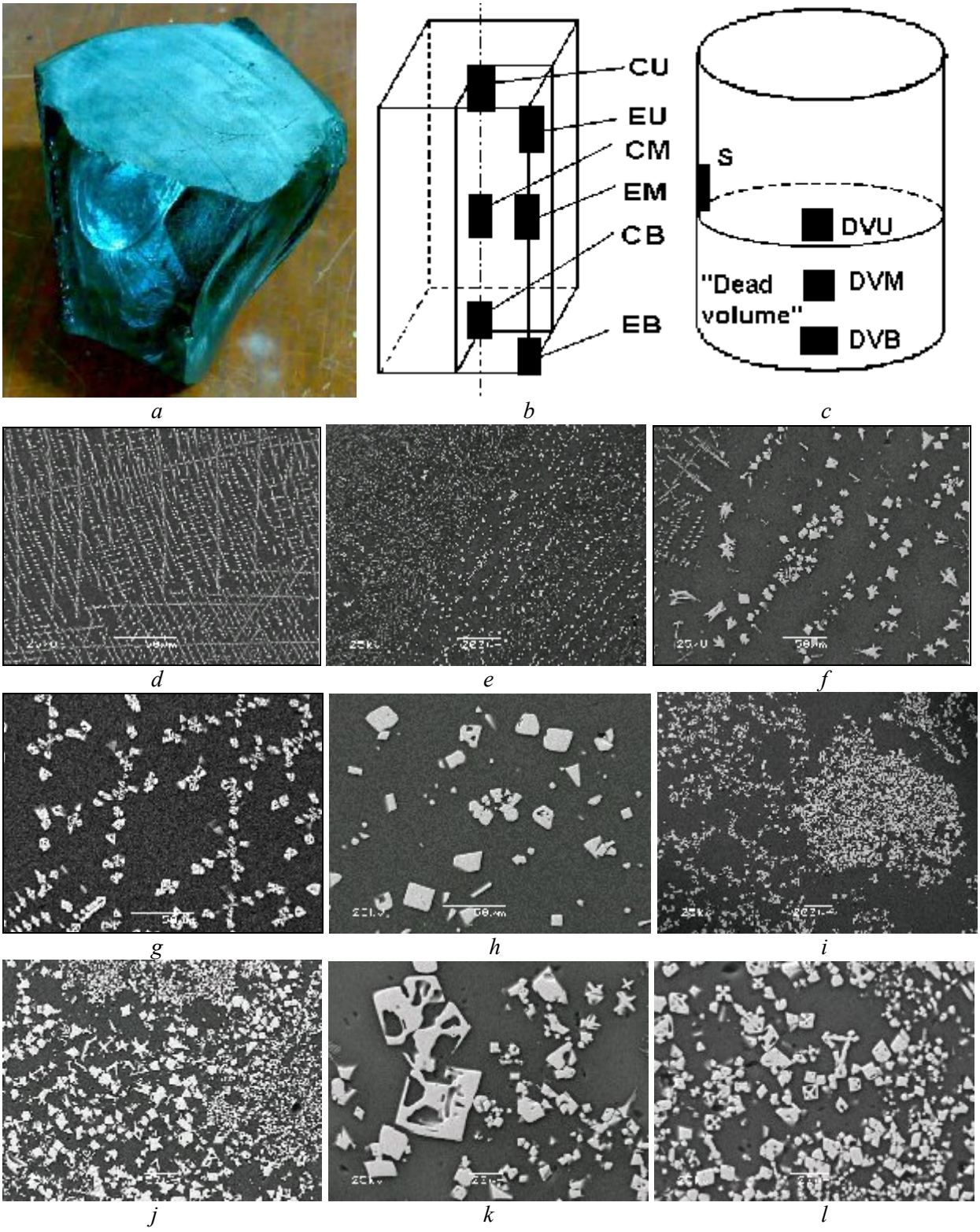

Figure 4. View of Piece of Glass Block (*a*) and Scematic View of a Section Cut Off from the Slowly Cooled Glass Block (*b*) and "Dead" Volume in the Cold Crucible (*c*) and Sampling Areas and SEM Images of the glassy materials sampled from molds (d-f) and canisters (g-l). See explanations in the text. C – core, E – edge, U – upper part, M – middle part, B – botom part, S – "skull", DV – "dead volume".

Table VII. Chemical Compositions (wt.%) of Co-Existing Phases in the Samples from Canister #4.

Oxide	CU			CM			CB			EU		EM			EB		
	Scan	V	S+V	Scan	V	S	Scan	V	S	V	S+V	Scan	V	S+V	Scan	V	S+V
Na_2O	13.39	14.94	5.13	13.26	13.58	-	14.58	14.66	-	13.02	6.00	12.75	15.41	11.78	15.87	15.58	9.67
MgO	1.77	1.61	2.57	1.86	1.41	2.50	1.44	1.29	2.98	1.29	2.41	1.66	1.50	1.76	2.23	1.52	2.26
Al_2O_3	17.06	19.15	7.71	18.60	18.08	2.10	17.89	19.07	1.89	18.87	8.90	17.11	20.2	16.64	18.46	20.85	10.52
SiO_2	34.81	41.05	12.00	35.06	39.31	*0.83*	34.46	41.8	-	40.77	13.37	37.2	41.58	33.69	38.51	43.34	16.86
SO_3	-	0.30	-	*0.51*	-	-	0.36	0.26	-	0.14	*0.01*	-	*0.35*	-	*0.25*	-	-
Cl	0.31	0.47	-	0.28	0.37	-	0.55	0.55	-	0.49	*0.15*	0.46	0.39	-	0.25	0.48	-
K_2O	*0.16*	*0.13*	-	*0.20*	-	-	-	-	-	*0.04*	-	-	-	-	*0.17*	0.17	-
CaO	1.99	2.38	0.65	1.91	2.11	-	1.55	2.19	-	2.37	0.71	1.95	2.39	2.08	1.96	2.23	0.84
Cr_2O_3	*0.15*	-	*0.25*	*0.17*	-	0.86	-	-	1.40	-	0.43	-	-	-	*0.11*	-	0.36
MnO	3.33	2.36	6.92	3.09	2.49	7.17	2.89	2.50	7.92	2.59	6.62	3.05	2.71	3.36	3.26	2.55	6.75
Fe_2O_3	14.35	4.80	55.71	11.45	5.09	67.59	11.60	5.42	73.02	4.64	56.46	15.02	6.75	20.63	15.01	4.26	56.68
NiO	0.64	-	1.70	*0.19*	-	3.78	*0.29*	-	4.93	-	3.51	0.53	-	-	0.57	-	1.72
CuO	-	-	-	*0.26*	-	-	*0.27*	-	-	-	*0.04*	-	-	-	-	-	-
ZnO	-		*0.33*	-	-	*0.19*	-	-	-	-	*0.03*	*0.28*	-	-	-	-	-
Cs_2O	*0.19*	0.51	-	0.54	0.40	-	0.64	0.29	-	*0.26*	0.36	*0.24*	0.26	-	0.44	*0.13*	-
PbO	*0.32*	*0.20*	-	*0.22*	-	-	0.22	-	-	*0.26*	*0.20*	-	-	-	0.23	-	-
Total	88.47	87.90	92.97	87.60	82.84	85.02	87.00	88.03	92.14	84.74	99.20	90.25	91.54	89.94	97.50	91.11	105.66

Table VIII. Chemical Compositions (wt.%) of Co-Existing Phases in the Samples from Canister #5.

Oxide	CU		CM		CB		EU		EM			EB	
	V	S+V	V	S+V	V	S	V	S	Scan	V+S	S+V	V	S+V
Na_2O	12.62	6.42	12.05	7.12	11.83	-	12.67	-	12.94	12.48	11.38	12.53	10.12
MgO	1.47	2.42	1.45	2.51	1.40	2.37	1.44	2.85	1.60	1.30	1.61	1.36	1.70
Al_2O_3	18.29	8.76	17.57	9.02	17.07	3.87	18.9	2.92	17.04	17.37	16.20	17.35	14.31
SiO_2	39.49	14.71	38.62	28.55	37.75	-	41.03	-	35.00	36.93	33.56	36.61	30.04
SO_3	*0.13*	-	*0.17*	*0.04*	0.15	-	*0.14*	-	*0.15*	*0.14*	-	*0.10*	-
Cl	0.49	-	0.33	*0.20*	0.46	-	0.53	-	0.39	0.38	0.39	0.53	0.37
K_2O	*0.07*	-	*0.05*	*0.02*	*0.04*	-	-	-	*0.04*	*0.09*	*0.12*	*0.04*	-
CaO	2.24	0.78	2.18	0.80	2.04	-	2.46	-	1.86	1.97	1.58	1.49	1.57
Cr_2O_3	-	0.28	*0.06*	0.30	-	1.17	-	1.03	*0.11*	*0.03*	-	-	*0.05*
MnO	2.37	6.18	2.42	6.64	2.48	6.48	2.50	8.34	3.34	3.02	3.67	2.76	3.48
Fe_2O_3	4.24	52.85	5.20	35.8	5.50	74.60	5.06	80.62	15.62	11.68	21.27	6.91	23.68
NiO	-	3.14	0.31	3.11	-	11.46	-	4.23	0.81	0.46	1.32	-	2.01
CuO	-	*0.03*	-	*0.05*	-	*0.03*	-	*0.02*	*0.02*	*0.02*	*0.05*	-	*0.01*
ZnO	-	*0.01*	-	*0.03*	-	*0.02*	-	*0.30*	*0.03*	*0.02*	*0.05*	-	*0.02*
Cs_2O	*0.24*	*0.01*	0.33	-	*0.21*	-	0.56	-	0.71	0.27	*0.27*	*0.23*	*0.15*
PbO	*0.23*	-	*0.25*	-	*0.21*	-	*0.06*	-	*0.20*	0.22	-	*0.20*	*0.51*
Total	81.87	95.54	80.99	94.19	79.14	100.00	85.35	100.00	89.86	86.38	91.47	80.11	88.92

Samples from "Dead Volume" and "Skull"

In the upper (DVU) and middle (DVM) parts of the "dead volume" individual spinel crystals form agglomerates non-uniformly distributed in the matrix vitreous phase (Fig. 4*j*). Dendrite-type crystals do

not occur. Average degree of crystallinity for the DVU and DVM samples may be estimated as 17-19 vol.% and 19-22 vol.%, respectively. Within the agglomerates the degree of crystallinity is much higher and may achieve ~30 vol.% (Fig. 4*h*) in the DVU and up to 45 vol.% in the DVM samples Fig. 4*k*). Individual spinel crystals have size of up to 25-30 μm across. These large crystals were formed at slow

Table IX. Chemical Compositions (wt.%) of Co-Existing Phases in the Samples from Canister #6.

Oxide	CU			CM		CB		EU				EM	EB	
	Scan	V	S+V	V	S	V	S	Scan	V	S-1	S-2	Scan	V	S
Na_2O	11.80	11.21	3.20	12.08	-	11.8	-	12.81	10.14	-	-	12.68	11.73	-
MgO	1.43	1.21	2.51	1.28	2.40	1.13	2.42	1.27	1.38	2.06	2.50	1.49	1.45	2.77
Al_2O_3	16.84	17.12	5.59	18.37	4.85	17.57	3.70	16.61	16.34	5.70	2.97	16.84	18.27	4.28
SiO_2	35.09	36.67	6.50	40.23	-	37.87	-	34.78	35.40	-	-	35.00	40.23	-
SO_3	*0.14*	*0.13*	*0.05*	*0.12*	-	*0.11*	-	*0.13*	*0.14*	-	-	*0.14*	*0.13*	-
Cl	0.46	0.49	-	0.55	-	0.51	-	0.46	0.52	-	-	0.52	0.47	-
K_2O	*0.04*	*0.11*	-	*0.12*	-	*0.09*	-	*0.05*	*0.07*	-	-	*0.06*	*0.08*	-
CaO	1.69	1.96	0.33	2.14	-	2.11	-	1.82	2.31	-	-	1.77	2.34	-
Cr_2O_3	*0.11*	-	0.51	-	1.30	-	1.80	0.22	-	3.83	0.79	*0.12*	-	2.88
MnO	2.80	2.06	6.34	2.25	6.20	2.46	6.00	2.95	2.50	5.79	7.34	3.26	2.26	5.72
Fe_2O_3	13.13	4.55	61.51	4.87	72.90	6.55	72.75	14.46	5.85	68.86	80.46	16.9	3.84	70.50
NiO	0.51	-	3.67	-	12.28	-	13.21	0.80	-	13.76	5.95	0.8	-	13.70
CuO	*0.03*	-	*0.03*	-	*0.03*	-	*0.07*	0.03	-	-	-	*0.03*	-	0.07
ZnO	*0.03*	-	*0.04*	-	*0.04*	-	*0.06*	0.03	-	-	-	*0.03*	-	0.08
Cs_2O	*0.20*	*0.34*	-	0.61	-	0.43	-	0.34	0.38	-	-	*0.44*	0.41	-
PbO	*0.48*	*0.22*	*0.12*	*0.23*	-	*0.23*	-	*0.24*	*0.24*	-	-	*0.24*	0.29	-
Total	84.78	76.07	90.40	82.85	100.00	80.86	100.00	87.00	75.27	100.00	100.00	90.40	81.50	100.00

Table X. Chemical Compositions (wt.%) of Co-Existing Phases in the Samples from Canister #7.

Oxide	CU		CM			CB			EU		EM		EB	
	V	S	Scan	V	S	Scan	V	S	Scan	V	Scan	F	V	S
Na_2O	12.47	-	13.25	11.03	-	12.34	11.26	-	11.49	12.21	10.97	-	11.62	-
MgO	1.06	2.04	1.49	1.43	2.80	1.33	1.36	2.13	1.10	1.39	1.60	9.47	1.07	2.26
Al_2O_3	18.15	4.95	17.54	17.97	3.34	17.66	17.1	3.32	15.57	16.96	16.17	0.68	17.3	5.96
SiO_2	39.65	-	36.22	39.73	-	35.22	37.44	-	31.61	37.85	32.57	30.04	37.94	-
SO_3	*0.14*	-	*0.14*	*0.14*	-	*0.14*	*0.15*	-	*0.15*	*0.14*	*0.14*	-	*0.14*	-
Cl	0.49	-	0.42	0.48	-	0.44	0.39	-	0.46	0.37	0.39	-	0.44	-
K_2O	*0.18*	-	*0.14*	*0.09*	-	*0.06*	*0.05*	-	*0.05*	*0.06*	0.14	-	*0.13*	-
CaO	1.47	-	1.98	2.18	-	1.98	2.27	-	1.75	1.99	1.70	0.68	1.97	-
Cr_2O_3	-	2.12	*0.12*	-	0.48	*0.13*	-	0.70	*0.12*	-	*0.12*		-	1.84
MnO	2.08	5.96	2.89	2.45	8.10	2.97	2.33	6.90	3.2	2.21	3.04	12.13	2.22	6.24
Fe_2O_3	5.52	71.77	12.55	4.87	79.24	12.15	6.40	77.77	14.6	4.28	15.11	45.42	4.19	70.60
NiO	-	13.03	0.64	-	6.03	0.41	-	9.07	0.87	-	0.93	1.57	-	12.66
CuO	-	0.06	0.02	-	-	*0.03*	-	*0.05*	*0.03*	-	*0.03*	-	-	*0.05*
ZnO	-	0.07	0.03	-	-	*0.03*	-	*0.08*	*0.03*	-	*0.03*	-	-	*0.38*
Cs_2O	0.50	-	0.52	*0.25*	-	0.49	*0.35*	-	0.49	0.26	*0.13*	-	0.42	-
PbO	*0.15*	-	*0.28*	*0.23*	-	*0.21*	*0.30*	-	*0.39*	0.31	*0.27*	-	*0.22*	-
Total	81.86	100.00	88.23	80.85	100.00	85.59	79.70	100.00	81.91	78.03	83.34	100.00	77.66	100.00

cooling in the bulk of the "dead volume". Due to quite large size of spinel crystals their chemical composition may be determined precisely (Table XI). As expected, Fe, Mn and Ni oxides are major components of the spinel phase and Cr, Mg and Al are minor components. Chemical composition of spinel crystals is some variable.
Matrix vitreous phase is not fully uniform and consists of lighter areas with higher Fe content and darker areas with lower Fe content (Table X). Formation of two glasses with slightly different chemical composition may be explained by melt stratification at interaction of "fresh" melt with colder melt in the "dead volume" in the cold crucible. In the middle part of the "dead volume" this phenomenon is absent (Table XI).

Table XI. Chemical Compositions (wt.%) of Co-Exising Phases from Upper (DVU), Middle (DVM) and Bottom (DVB) Parts of the "Dead Volume", and "Skull".

Oxide	DVU			DVM		DVB		Skull	
	LG	DG	S	V	S	Scan	V	V	S
Na_2O	12.92	13.69	-	15.47	-	12.29	14.46	15.82	-
MgO	1.87	1.63	2.92	1.59	2.87	2.57	2.01	1.20	3.25
Al_2O_3	19.17	18.69	4.49	20.58	4.01	21.16	23.14	20.70	3.30
SiO_2	40.20	42.07	-	43.06	-	34.44	40.22	44.49	-
SO_3	-	*0.36*	-	0.65	-	*0.21*	-	0.87	-
Cl	0.72	0.65	-	-	-	-	-	*0.25*	-
K_2O	-	-	-	-	-	*0.12*	-		-
CaO	2.55	2.40	-	2.15	-	2.18	2.76	1.99	-
Cr_2O_3	-	-	1.58	-	2.23	*0.15*	-	-	1.44
MnO	2.42	2.38	7.69	2.24	7.20	3.56	3.60	2.01	8.32
Fe_2O_3	8.70	6.78	67.75	4.99	71.41	16.85	8.33	7.48	72.80
NiO	-	-	6.45	-	6.84	0.83	-	-	7.81
CuO	-	-	*0.06*	-	*0.05*	*0.03*	-	-	0.04
ZnO	-	-	*0.05*	-	*0.05*	*0.03*	-	-	0.04
Cs_2O	0.59	0.43	-	*0.32*	-	0.43	-	0.63	-
PbO	-	-	-	*0.29*	-	*0.25*	-	*0.27*	-
Total	89.14	89.08	90.99	91.34	94.66	95.10	94.52	95.70	97.00

The glassy material from the near-"skull" zone is non-uniform and composed of agglomerates of fine individual spinel crystals and vireous matrix. Their size is widely varied – from several microns to ~15-20 μm (Fig. 5*l*). There are layers filled with fine (submiron-sized) spinel crystals and other inhomogeneities. Average degree of crystallinity was estimated to be 25-30 vol.%. XRD pattern of the material from the near-"skull" zone shows also occurrence of halite and minor hematite which were not revealed on SEM images.

CONCLUSIONS

Both the CCIM process parameters and glass melt and product structure and properties depends strongly on waste loading in glass especially content of crystalline phase in glass. The only crystalline phase in the SB4 waste glass is spinel whose content increases with waste loading in the glass. At relatively low waste loading (~50 wt.%) spinel content is low (<5 vol.%) and glass may be considered as a Newtonian liquid obeying the Frenkel-Andrade law. Spinel content increases to ~6-8 vol.% at 55 wt.% waste loading and to ≥12 vol.% at 60 wt.% waste loading. At that appreciable deviation from the Frenkel-Andrade law takes place. This may effect on crystal settling/formation in waste-bearing borosilicate melts. Neverheless, at constant waste loading (55 wt.%) variation of melt residence time in the cold crucible from 30 to 90 min

nearly does not effect on crystal settling/formation neither in the as-poured nor slowly cooled glassy materials. All the materials produced were composed of vitreous and spinel structure phases. Chemical composition of spinel corresponds to trevorite/magnetite solid solution. Spinel forms both dendrite (skeleton-type aggregates) of fine (micron- or submicron-sized) crystals segregated at early stages of melt solidification and larger (up to tens of microns) individual more regular crystals formed during slow melt cooling. High content of micron- or submicron-sized dendrite (skeleton-type) spinel crystals in some specimens increases apparent degree of crystallinity and as a result of which zones cooled at higher rate look higher crystallized that those cooled at lower rate. Specific dependence of elemental distribution within the glass blocks has not been brought out, but here is a tendency to elemental separation in the glass blocks with enrichment of the deeper zones with heavier transition metal ions and their depletion with Na, Cs, Ca, Al, Si.

ACKNOWLEDGEMENTS

The work was performed under financial support from US DOE Office of Environmental Management. Special thanks to Dr. K.D. Gerdes.

REFERENCES

1. A.P. KOBELEV, S.V. STEFANOVSKY, V.V. LEBEDEV, M.A. POLKANOV, V.V. GORBUNOV, A.G. PTASHKIN, O.A. KNYAZEV, J.C. MARRA, K.D. GERDES, “Full-Scale Cold Crucible Test on Vitrification of Savannah River Site SB4 HLW Surrogate,” The MS&T 2008 /ACerS 110th Annual Meeting, October 5-9, 2008, Pittsburgh, PA. Paper ID 485985 (2009).
2. S.V. STEFANOVSKY, A.P. KOBELEV, V.V. LEBEDEV, M.A. POLKANOV, D.Y. SUNTSOV, J.C. MARRA, “The Effect of Waste Loading on the Characteristics of Borosilicate SRS SB4 Waste Glasses,” ICEM ’09/DECOM ’09: 12th International Conference on Environmental Remediation and Radioactive Waste Management. October 11-15, 2009, Liverpool, UK. CD-ROM (2009)
3. J.C. MARRA, “Sludge and Glass Compositions for Cold Crucible Induction Melter (CCIM) Testing – Sludge Batch 4,” SRT-MST-2007-00070, Savannah River National Laboratory (2007).
4. S.L. MARRA and C.M. Jantzen, “Characterization of Projected DWPF Glasses Heat Treated to Simulate Canister Centerline Cooling (U).” Westinghouse Savannah River Co. WSRC-TR-92-142, Rev. 1 (1993).
5. I.Ya. ZALKIND, V.S. VDOVICHENKO and E.P. DICK, “Ashes and Slags in Incinerators,” (Russ.) Moscow (1988).